Proceedings of COBEM 2005

18th International Congress of Mechanical Engineering
November 6-11, 2005, Ouro Preto, MG

A STRESS BASED H-ADAPTIVE TOPOLOGY OPTIMIZATION METHOD

João. Carlos Arantes. Costa Jr.
Dep. Mechanical Eng., UFRN, CEP 59072-970, Natal, RN, Brasil
arantes@ufrnet.br

Marcelo Krajnc Alves
Dep. Mechanical Eng., UFSC, CEP 88040-970, Florianópolis, SC, Brasil
krajnc@emc.ufsc.br

Hazim Ali Al-Qureshi
Dep. Mechanical Eng., Universidade Federal de Santa Catarina, Florianópolis, SC, 88010-970, Brazil
hazim@materiais.ufsc.br

Abstract. *This work proposes an optimization procedure that combines a stress based layout optimization with an h-refinement strategy, which is able to determine an optimal layout that is ready to be manufactured. In addition, the procedure generates a well-defined material/void interface; reduces considerably the size of the optimization problem, for a given resolution; and bound the relative solution error. In this research, the local stress constraints are transformed into a global stress measure reducing the computational cost in deriving the optimal layout. More importantly, the usage of the global stress measure together with the h-adaptive procedure results in an optimal layout that violates, with less than 2%, the local stress criterion.*

Keywords*: topology, layout, optimization; stress based,* h-*adaptive refinement*

1. Introduction

Since the introduction of the material distribution technique for the determination of the optimum layout of continuum structures, most of the work has been related to the minimization of a compliance type of design criteria. However, to obtain an optimum layout ready to manufacture, stress constraints must be considered. The major difficulties in stress based layout problems are:

- The necessity to consider a very large number of constraints, in order to correctly approximate the local parametric stress criterion. Notice that, for actual computation, these constraints must be evaluated at a series of discrete points, whose distribution should be dense enough in order to minimize the chance of any significant constraint violation between specified points.
- The requirement of robust and cost effective non-linear programming solvers, due to the highly nonlinear behavior of the stress constraints.

One way to avoid the usage of a very large number of constraints is to transform the local stress criteria into a global stress measure. The global stress measure is then implemented as a single constraint reducing considerably the computational cost required to solve the optimization problem. Different global measures have been applied in the scope of layout optimization problems. Among them are: the Kreisselmeir-Steinhauser and the Park-Kikuchi measures, see Yang and Chen (1996); the p-mean and p-norm measures, see Duysinx and Sigmund (1998). The disadvantage of the usage of the global measure approach is the weaker control of the local stress criteria. However, as we will verify in section 6, the proposed procedure leads to optimal layouts that violate, with less than 0.45%, the local stress criterion.

In addition, most layout optimization problems are based on a "pixel" approach where a fixed refined rectangular mesh is employed. Consequently, to obtain a well-defined material contour (material/void interface) it is necessary to employ a small "pixel" size, which increases dramatically the number of design variables to be optimized. Different methods were proposed with the aim of reducing the size of the layout problem. Among these methods are the evolutionary structural optimization methods, see Querin *et al.* (2000) and Reynolds (2000) *et al.*. The drawback of these methods is that they use a hard-kill strategy that is greatly influenced by the addition/removal ratio, which cannot be determined effectively. A different approach is the solution of a layout optimization followed by a shape optimization procedure. Here, the difficulty occurs in the process that automatically identifies the contour of the resulting layouts. Recently, a new approach that combines layout optimization with *h*-refinement strategies was proposed, Costa and Alves (2003). Additional references about adaptive refinement may be found in Costa (2003).

Here, we present an optimization method, based in Costa and Alves (2003), that is able to generate, automatically, a ready to manufacture optimal layout, with a well-defined material contour. The proposed procedure consists in the solution of a sequence of layout optimizations followed by a one step *h*-refinement procedure, where we can see that the element size of the final optimal layout defines the resolution of the final contour.

The layout optimization problem minimizes the mass of a body subjected to a local stress failure criterion and whose design variables are submitted to side and slope constraints. Now, let Ω represent the body domain with boundary $\partial\Omega = \Gamma_u \cup \Gamma_t$, $\Gamma_u \cap \Gamma_t = \varnothing$, where Γ_u denotes the part of the boundary with a prescribed displacement, i.e. $\boldsymbol{u} = \bar{\boldsymbol{u}}$, and Γ_t denotes the part of the boundary with a prescribed traction load, i.e. $\sigma \boldsymbol{n} = \bar{\boldsymbol{t}}$. Also, let $\bar{\boldsymbol{b}}$ represent the prescribed body force defined in Ω, $H_o = \left\{ v_i \in H^1(\Omega)^2 \middle| \boldsymbol{v} = 0 \text{ on } \Gamma_u \right\}$ and $H = \{H_o + \bar{\boldsymbol{u}}\}$ denote respectively the sets of admissible variations and displacements. Then, the weak formulation of the problem, defining the state equation, may be stated as: Find $\boldsymbol{u} \in H(\Omega)$ such that

$$a(\boldsymbol{u},\boldsymbol{v}) = l(\boldsymbol{v}), \quad \forall\, \boldsymbol{v} \in H_o \tag{1}$$

where

$$a(\boldsymbol{u},\boldsymbol{v}) = \int_\Omega D^H(\rho)\varepsilon(\boldsymbol{u})\cdot\varepsilon(\boldsymbol{v})\,d\Omega \text{ and } l(\boldsymbol{v}) = \int_\Omega \boldsymbol{b}\cdot\boldsymbol{v}\,d\Omega + \int_{\Gamma_t} \boldsymbol{t}\cdot\boldsymbol{v}\,d\Gamma\,. \tag{2}$$

Here, ρ is the relative density and $\boldsymbol{\varepsilon}(\circ)$ is the operator defined by: $\boldsymbol{\varepsilon}(\circ) = \frac{1}{2}\left(\nabla(\circ) + \nabla(\circ)^T\right)$.

2. Definition of the material model

The solution of the layout/topology optimization problem makes use of the material approach, which considers a porous material characterized by its relative density. The modeling of its effective properties, at intermediate densities, uses the SIMP model; see Bendsoe and Sigmund (1999), where the effective Young's modulus is given by

$$E(\rho) = \rho^\eta E_0\,. \tag{3}$$

Here, E_0 is the Young's modulus, relative to the fully dense material, and η is a penalty parameter, given by η=4.

To establish a stress criterion for this model, at intermediate densities, it is necessary to introduce an effective stress measure, which penalizes intermediate density regions, associated with a composite material result. Here, the effective stress measure $\sigma^*(\rho)$, proposed by Duysinx and Sigmund (1998) and Duysinx and Bendsoe (1998), is given by:

$$\sigma^*(\rho) = \frac{\sigma(\rho)}{\rho^\eta}\,. \tag{4}$$

Now, using Eq.(4) and the von Mises failure criterion, we can express the stress constraint as:

$$\sigma^*_{eq}(\rho) = \frac{\sigma_{eq}(\rho)}{\rho^\eta} \le \sigma_y\,, \text{ with } \sigma_y \text{ - yield stress} \tag{5}$$

ε-Relaxed stress criterion

A major difficulty in layout optimization with stress constraints is caused by the "singularity phenomenon", due to the degeneracy of the design space. In order to handle this difficulty, Cheng and Guo (1997) applied a perturbation method, denoted the ε-relaxation technique. This strategy replaces the solution of the "singular" problem by the solution of a sequence of perturbed non-singular problems. Here, the modified ε-relaxed stress criterion is given by:

$$\rho\left(\frac{\sigma^*_{eq}(\rho)}{\sigma_y} - 1\right) - \varepsilon(1-\rho) \le 0\,. \tag{6}$$

It is important to notice that, in order for a machine part to be ready to manufacture, it is necessary that the point wise ε-relaxed stress failure criterion be satisfied in all points of the body domain.

3. Definition of the material model

The problem consists of the determination of the relative density $\rho(x) \in W^{1,\infty}(\Omega)$, that solves:

$$\min \frac{1}{\Omega}\int_\Omega \rho(\boldsymbol{x})\,d\Omega \tag{7}$$

Subjected to:

- Stress constraints

$$\rho\left(\frac{\sigma^*_{eq}(\rho)}{\sigma_y}-1\right)-\varepsilon(1-\rho)\le 0, \quad \forall\ \boldsymbol{x}\in\Omega\,, \tag{8}$$

• Side constraints
The relative density $\rho(\boldsymbol{x})\in\left[\rho^{\inf},1\right]$, $\rho^{\inf}=0.001$. Thus,

$$\rho^{\inf}\le\rho(\boldsymbol{x})\le 1, \quad \forall\boldsymbol{x}\in\Omega\,, \tag{9}$$

• Stability constraints
In order to assure the existence of a solution to the optimal layout problem, avoid the occurrence of checkerboard instabilities and reduce the initial mesh dependency of the optimal layout, see Petersson and Sigmund (1998), we enforce a slope constraint, given by:

$$\left(\frac{\partial\rho}{\partial x}\right)^2\le C_x^2 \text{ and } \left(\frac{\partial\rho}{\partial y}\right)^2\le C_y^2 \tag{10}$$

The constants C_x and C_y impose a bound to the slope of the relative density field and are defined in section 3.

Integrated ε-relaxed stress constraint

Now, the ε-relaxed stress constraint, given in Eq.(6), has to be satisfied at all $\boldsymbol{x}\in\Omega$, which characterizes a parametric constraint. One effective method of handling a parametric constraint is to relax the point wise criterion by considering an integrated constraint. Here, we consider the following integrated ε-relaxed stress constraint:

$$\left\{\frac{1}{\Omega}\int_\Omega\left\langle\rho\left(\frac{\sigma^*_{eq}(\rho)}{\sigma_y}-1\right)-\varepsilon(1-\rho)\right\rangle^p d\Omega\right\}^{1/p}\le 0\,, \tag{11}$$

where $\langle f(\boldsymbol{x})\rangle$ defines the positive part of *f*, i.e., $\langle f(\boldsymbol{x})\rangle=\max\{0, f(\boldsymbol{x})\}$ and p=4.

4. Discretization of the problem

At this point we apply the Galerkin finite element method where we employ a *Tri3* finite element that interpolates both the displacement and the relative density fields. The main drawback is the presence of a layer of intermediate density material, along the material/void interface, which can be considerably minimized by using the proposed *h*-adaptive scheme. The design variables are defined as the relative density of material in each node of the mesh. Moreover, since the gradient of the relative density is constant within each element, it is only necessary to impose:

$$\left(\frac{\partial\rho}{\partial x}\right)^2_e\le\left(C_x^e\right)^2 \text{ and } \left(\frac{\partial\rho}{\partial y}\right)^2_e\le\left(C_y^e\right)^2, \tag{12}$$

where $e=1,...n_e$, with n_e representing the total number of elements in the mesh.

4.1. Determination of the bounds C_x^e and C_y^e

Now, consider a generic tri3 element where $\boldsymbol{x}_i=(x_i,y_i)$, i=1…3, are the coordinates of the vertices and $\boldsymbol{x}_m=(x_m,y_m)$ is the coordinate of the baricenter of the element. Let $\boldsymbol{d}_i=\left(x_i-x_m\right)\boldsymbol{e}_x+\left(y_i-y_m\right)\boldsymbol{e}_y$, then

$$d_{\min}=\min_{i=1,\dots 3}\left\|\boldsymbol{d}_i\right\|, \text{ then } C_x^e=C_y^e=\frac{1}{d_{\min}}. \tag{13}$$

A modification of the bounds, i.e. of C_x^e and C_y^e, must be performed if at least one of the sides of the element coincide with an axis of symmetry. Here, we consider two possible cases, which are:

• x - axis of symmetry*: In this case we must have:* $v = 0$ *and* $\frac{\partial \rho}{\partial y} = 0$ *, which is attained by setting* C_y^e *=0.*

• y - axis of symmetry*: In this case we must have:* $u = 0$ *and* $\frac{\partial \rho}{\partial x} = 0$ *, which is attained by setting* C_x^e *=0.*

A detailed explanation of the bounds is given in Costa (2003).

4.2. Formulation of the discrete problem

The discrete formulation of the layout optimization problem may be stated as: Determine $\boldsymbol{\rho} \in \mathbf{X}$, $\mathbf{X} = \left\{ \boldsymbol{\rho} \in \mathbb{R}^n \middle| \rho_i^{\inf} \le \rho_i \le 1, i = 1,...n \right\}$, that solves

$$\min f(\boldsymbol{\rho}) = \frac{1}{\Omega} \int_\Omega \rho \, d\Omega \tag{14}$$

subjected to:

$$h(\boldsymbol{\rho}, \boldsymbol{u}(\boldsymbol{\rho})) = \left\{ \frac{1}{\Omega} \int_\Omega \left\langle \rho \left(\frac{\sigma_{eq}^*(\rho)}{\sigma_y} - 1 \right) - \varepsilon (1-\rho) \right\rangle^p d\Omega \right\}^{1/p} \le 0, \tag{15}$$

$$g_{2e-1}(\boldsymbol{\rho}) = \frac{1}{\beta} \left\{ \left(\frac{\partial \rho}{\partial x} \right)_e^2 - \left(C_x^e \right)^2 \right\} \le 0, \text{ and } g_{2e}(\boldsymbol{\rho}) = \frac{1}{\beta} \left\{ \left(\frac{\partial \rho}{\partial y} \right)_e^2 - \left(C_y^e \right)^2 \right\} \le 0 . \tag{16}$$

Here $e = 1,...n_e$ and $\beta = \frac{1}{d_{\max}}$, with $d_{\max} = \max_{i=1,...3} \|\boldsymbol{d}_i\|$.

To solve the discrete optimization problem, we apply the Augmented Lagrangian method, reducing the problem to the solution of a sequence of box constrained minimization, which is solved by the MMA method, see Svanberg (1987).

5. Description of the combined method

5.1. Description of the procedure

Here, a general description of the procedure is presented that combines a stress based layout optimization with *h*-adaptive mesh refinement strategies, with the aim of:

- Generating a ready to manufacture optimal layout with a well-defined material contour (material/void interface) of the optimal layout.
- Reducing the initial mesh dependency of the optimal layout;
- Reducing considerably the size of the layout optimization for a prescribed refined resolution of the optimal topology;
- Decreasing the solution error of the state equation.

We set a priori the total number of *h*-refinement levels and solve, at each *h*-refinement step, a layout optimization problem, see Fig. 3. The procedure is described as:

• Initialize the design variables

• For each *h*-refinement level, do:

(i) Solve the layout optimization problem

(ii) Apply the mesh refinement procedure

(a) Perform the mesh refinement

(i) Identify which elements must be refined

(ii) Perform the refinement of the elements and introduce the necessary transition elements in order to maintain the mesh compatibility

(iii) Apply a constrained Laplacian smoothing procedure in order to improve the mesh quality

(b) Optimize the element nodal incidence for the profile reduction

5.2. Mesh Refinement Strategy

The strategy consists basically in: the identification of the set of elements to be refined; the refinement of these elements, as illustrated in Fig. 1; and the introduction of the transition elements necessary to maintain the mesh compatibility. In order to explain the criteria used in the determination of the set of elements to be refined, we introduce a pointer vector: *Pref(i),* $i=1,\ldots n_e$. The default value is *Pref(i)*=0, representing no refinement of the *i-th* element. However, if *Pref(i)*=1, then the *i-th* element belongs to the set of elements to be refined. The criteria, employed in the determination of the set of elements to be refined, are described as follows:

(i) Set *Pref(i)*=0, $i=1,\ldots n_e$.

(ii) For each element, we determine the relative density at the baricenter, i.e., $\rho_i^{bar}, i=1,\ldots n_e$. If $\rho_i^{bar} \geq 0.4$, the element is defined as a "material" element and we set: *Pref(i)*=1. Otherwise, the element is denoted a non-material element. Here, we define the material boundary to be given by the common interface of two elements, one being a material element and the other a non-material element. Notice that, at this step, we identify the "material" elements, which are all refined.

(iii) Determine the global and the elements average errors denoted respectively by Θ_G and Θ_E, $e=1,\ldots n_e$. Notice that, for each element we verify if $\Theta_E > (1+\varphi)\Theta_G$ for some given $\varphi > 0$. If true, we set *Pref(e)*=1, i.e., the *e-th* element will be refined. These error measures will be defined in section 5.4.

(iv) Determine the quality measure *Q* of each element in the mesh, given by

$$Q = \frac{6A}{\sqrt{3}\, L_{\max}\, P} \tag{17}$$

in which: *A* is the area of the triangle, *P* is the one half of the perimeter of the triangle and $L_{\max} = \max\{\overrightarrow{ab}, \overrightarrow{ac}, \overrightarrow{bc}\}$ is the length of the element's largest side. Thus, for each element we verify: if $Q(e) \leq 0.55$ then we set: *Pref(e)*=1.

(iv) Identify all the non-material elements that have a face common with the material contour and set their pointer reference *Pref(e)*=1. Thus, all non-material elements having a material element neighbor are also refined.

(v) Perform an additional smoothing refinement criterion. Here, for each element whose *Pref(e)*=0, we identify their neighbors. If the element has 2 or more neighbors whose *Pref(.)*=1, then we refine the given element, i.e., set *Pref(e)*=1. The objective here is to avoid having a given non-refined element with 2 or more neighbors that will be refined. This may generate sharp edges in the material contour or internal void regions with a poor material contour definition.

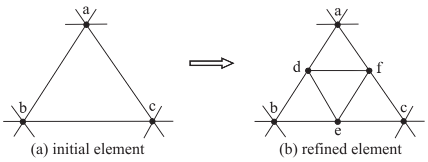

Figure 1. Scheme of refinement element.

5.3. Conditional Laplacian smoothing procedure

The mesh is improved with the application of a constrained Laplacian smoothing, as described in Fig. 2. Here, n_d is the number of adjacent nodes associated with node x_n.

The Laplacian process is conditional since it is only implemented if the mesh quality of the set of elements, with the modified coordinate of the center node, improves. The mesh quality of the set of elements is given by the quality of the worst element in the set. The measure of quality of a given element is given by Eq.(17).

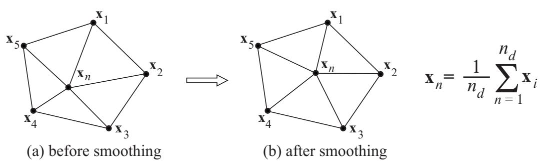

Figure 2. Scheme of refinement element.

5.4. Error estimator criteria

We consider an error estimator based on a gradient recovery technique by means of the energy norm. Let $\boldsymbol{\rho}$ be a given realizable nodal relative density vector, then, the local displacement error is: $\boldsymbol{e}(\boldsymbol{\rho}) = \boldsymbol{u}(\boldsymbol{\rho}) - \boldsymbol{u}^h(\boldsymbol{\rho})$, where $\boldsymbol{u}(\boldsymbol{\rho})$ and $\boldsymbol{u}^h(\boldsymbol{\rho})$ are the exact and approximate solution respectively. The energy norm is given by:

$$\|e(\boldsymbol{\rho})\|_{\mathrm{E}}^{2} = \int_{\Omega} D^{H}(\boldsymbol{\rho})\varepsilon\left(\mathbf{e}(\boldsymbol{\rho})\right)\cdot\varepsilon\left(\mathbf{e}(\boldsymbol{\rho})\right)d\Omega . \tag{18}$$

As a result, the local stress error may be expressed as:

$$\|\mathbf{e}(\boldsymbol{\rho})\|_{\mathrm{E}}^{2} = \int_{\Omega}\left(\sigma(\boldsymbol{\rho})-\sigma^{h}(\boldsymbol{\rho})\right)\cdot\left[D^{H}(\boldsymbol{\rho})\right]^{-1}\left(\sigma(\boldsymbol{\rho})-\sigma^{h}(\boldsymbol{\rho})\right)d\Omega , \tag{19}$$

where $\sigma(\boldsymbol{\rho})-\sigma^{h}(\boldsymbol{\rho}) = D^{H}(\boldsymbol{\rho})\varepsilon\left(\boldsymbol{u}(\boldsymbol{\rho})-\boldsymbol{u}^{h}(\boldsymbol{\rho})\right)$, with $\sigma^{h}(\boldsymbol{\rho})$ denoting the approximate stress field, derived by a given nodal density vector $\boldsymbol{\rho}$. Now, since the exact stress distribution is unknown, we approximate the exact stress, $\sigma(\boldsymbol{\rho})$ **,** by an improved solution $\sigma^{*}(\boldsymbol{\rho})$, which is more accurate than $\sigma^{h}(\boldsymbol{\rho})$. The improved solution, $\sigma^{*}(\boldsymbol{\rho})$, is determined by minimizing the potential $\psi(\boldsymbol{\rho})$, given by

$$\psi(\boldsymbol{\rho}) = \int_{\Omega}\left(\sigma^{*}(\boldsymbol{\rho})-\sigma^{h}(\boldsymbol{\rho})\right)\cdot\left(\sigma^{*}(\boldsymbol{\rho})-\sigma^{h}(\boldsymbol{\rho})\right)d\Omega . \tag{20}$$

Once $\sigma^{*}(\rho)$ is determined, we may compute the global and element average errors, Θ_{G} and Θ_{E}, and given by:

$$\Theta_{\mathrm{G}} = \frac{1}{\Omega}\int_{\Omega}\left(\sigma(\rho)-\sigma^{h}(\rho)\right)\cdot\left[D^{H}(\rho)\right]^{-1}\left(\sigma(\rho)-\sigma^{h}(\rho)\right)d\Omega \tag{21}$$

and

$$\Theta_{\mathrm{E}} = \frac{1}{\Omega_{\mathrm{E}}}\int_{\Omega_{\mathrm{E}}}\left(\sigma^{*}(\rho)-\sigma^{h}(\rho)\right)\cdot\left[D^{H}(\rho)\right]^{-1}\left(\sigma^{*}(\rho)-\sigma^{h}(\rho)\right)d\Omega_{\mathrm{E}} \tag{22}$$

6. Problem cases

We present some problem cases with the objective of attesting the performance of the proposed method. With the aim of showing the evolution of the *h*-refinement strategy, we illustrate the intermediate optimal layouts, meshes and point-wise distribution of the ε-relaxed stress criterion.

For simplicity, a unique material is used in all problem cases where the Young's Modulus E_0=215.0 GPa, the Poisson's ratio $\nu_0 = 0.3$ and σ_y=260.0 MPa.

6.1. Problem case(1):

Here, we consider a slab clamped at the left and right edges and subjected to a distributed load *P*=259,999.0 kN/m at the middle of the top edge, as illustrated in Fig. 3a. The initial mesh, shown in Fig. 3a, has 1776 elements and 949 nodes. The second refined mesh had 4136 elements and 2149 nodes and finally, the final refined mesh, shown in Fig. 4a, has 10995 elements and 5610 nodes.

The evolution of the partial optimal layouts showing the improvement of the resolution of the material contour is illustrated in Fig. 3b and 4b; and the distribution of the ε-relaxed stress criterion is illustrated in Fig. 3c and 4c. Here, we can verify that the final optimal layout, shown in Fig. 4c, has violated the point-wise ε-relaxed stress criterion by 0.35%. Also, we can see that the sequence of optimal layouts tends to converge to a final optimal layout having a sharp material contour, satisfying a point-wise ε-relaxed stress criterion.

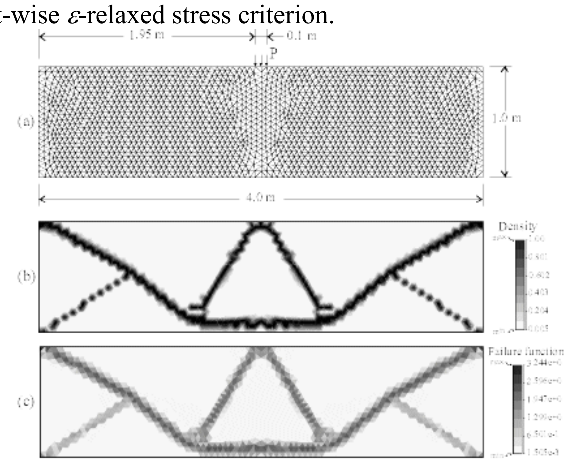

Figure 3. Initial mesh case (1): (a) mesh with 1776 elements and 949 nodes; (b) optimum layout; (c) failure function.

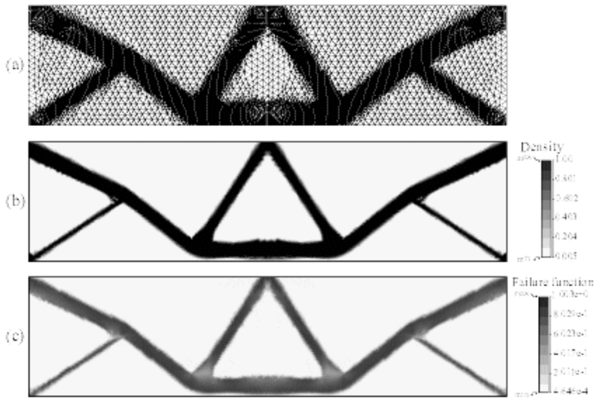

Figure 4. Third mesh case (1): (a) mesh with 10995 elements and 5610 nodes; (b) optimum layout; (c) failure function.

6.2. Problem case(2):

Here, we consider a slab subjected to a distributed load *P*=259,999.0 kN/m at the left and right edges, as illustrated in Fig. 5a. The initial mesh, shown in Fig. 5a, has 837 elements and 463 nodes. A second refined mesh, not shown here, used 2048 elements and 1078 nodes. A third refined mesh, not shown here, had 5629 elements and 2880 nodes and, finally, the last refined mesh shown in Fig. 6a has 16674 elements and 8420 nodes.

The evolution of the partial optimal layouts showing the improvement of the resolution of the material contour is illustrated in Fig. 5b and 6b. The evolution of the distribution of the ε-relaxed stress criterion is shown in Fig. 5c and 6c. Here, the final optimal layout has violated the point-wise ε-relaxed stress criterion by 0.45%.

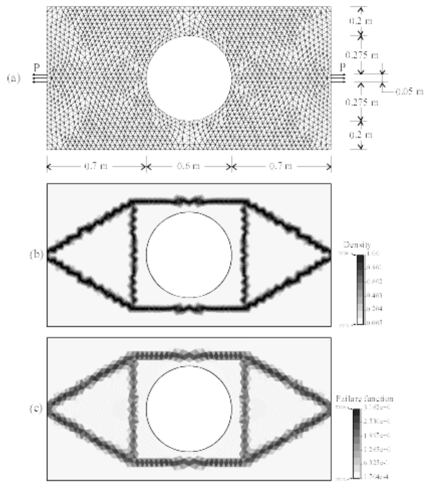

Figure 5. Initial mesh case (1): (a) mesh with 837 elements and 463 nodes; (b) optimum layout; (c) failure function.

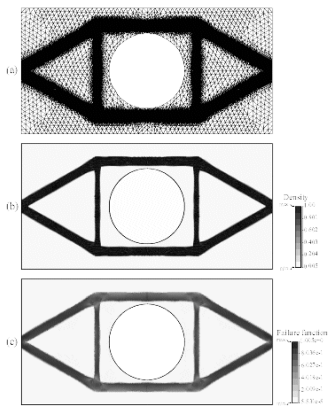

Figure 6. Fourth mesh case (2): (a) mesh with 16674 elements and 8420 nodes; (b) optimum layout; (c) failure function.

7. Conclusions

The proposed method has shown to be very effective and robust in generating a ready to manufacture optimal layout with a well-defined material contour. In addition, the procedure not only reduced considerably the size of the layout problem, for a given final optimal topology, but also bounded the solution error of the state equation.

It is important to emphasize that even though the procedure has generated a final optimal layout with up to 0.45% of violation of the point-wise ε-relaxed stress criterion, the results in all the problem cases investigated suggest that the sequence of optimal layouts tends to converge to an optimal layout that satisfies the point-wise ε-relaxed stress failure criterion. Moreover, the consideration of a low order interpolation for the finite element and the usage of a global stress measure have reduced dramatically the computational cost in deriving an optimal layout.

The proposed approach resulted in a very promising tool for the determination of a ready to manufacture optimal layout of machine parts. This goal is of fundamental importance in making layout optimization tools commercially viable for industrial usage. It is evident that no one can forecast the magnitude of this type of design tool, developed in this paper, but it is clear that all segments of the production system could take full advantage of the proposed technique.

In this work we have seen that the optimal topologies have given approximate truss like structures, approaching a fully stress design solution, as expected. In problem case 2, the optimal topologies have avoided curved results, tangent to the hole, which would be responsible for extremely large bending stresses. Moreover, both results satisfied, as a convergence criterion, the Kuhn Tucker necessary optimality condition.

Notice that the ε-relaxation is a continuation method so the exact solution is only obtained for $\varepsilon \to 0$. However, in practice, a sufficient small relaxation parameter is employed or a finite sequence of decreasing relaxation parameters is solved. Here, due to time limitations, we have considered a fixed value for the ε-relaxation.

A more detailed explanation to this work is presented in Costa (2003).

8. Acknowledgements

The authors wish to thank Prof. Krister Svanberg, from the Royal Institute of Tech., for providing the MMA solver.

9. References

Bendsoe M.P. and Sigmund O., 1999, Material Interpolation Schemes in Topology Optimization, Archive of Applied Mechanics 69 635-654.

Cheng G.D. and Guo X., 1997, ε-Relaxed Approach in Structural Topology Optimization, Struc. Optim. 13 258-266.

Costa Jr. J.C.A. and Alves M.K., 2003, Layout Optimization with *H*-adaptivity of Structures, Int. J. Numer. Meth. Engng. 58(1) 83-102.

Costa Jr. J.C.A., Otimização topológica com Refinos H-adaptativos, Universidade Federal de Santa Catarina, Florianópolis, Brazil, 2003.

Duysinx P. and Sigmund O., 1998, New Development in Handling Stress Constraints in Optimal Material Distribution, American Institute of Aeronautics and Astronautics, paper 98-4906.

Duysinx P. and Bendsoe M.P., 1998, Topology Optimization of Continuum Structures with Local Stress Constraints, Int. J. Numer. Meth. Engng. 43 1453-1478.

Petersson J. and Sigmund O., Slope Constrained Topology Optimization, Int. J. Numer. Meth. Engng. 41 1998 1417-1434.

Querin O.M., Young V., Steven G.P. and Xie Y.M., 2000, Computational Efficiency and Validation of Bi-directional Evolutionary Structural Optimization. Comput. Meth. Appl. Mech. Engng. 189 559-573.

Reynolds D., McConnachie J., Bettess P., Christie W.C. and Bull J.W., 1999, Reverse Adaptivity – A New Evolutionary Tool for Structural Optimization, Int. J. Numer. Meth. Engng. 45 529-552.

Svanberg K., The Method of Moving Asymptotes – A New Method for Structural Optimization, Int. J. Numer. Meth. Engng. 24 1987 359-373.

Sigmund O. and Petersson J., 1998, Numerical Instabilities in Topology Optimization: A Survey on Procedures Dealing with Checkerboards, Mesh Dependencies And Local Minima, Structural Optimization 16(1) 68-75.

Yang R.J. and Chen C.J., 1996, Stress-Based Topology Optimization, Structural Optimization 12 98-105.

10. Responsibility notice

The authors are the only responsible for the printed material included in this paper.